

# Image Cover Sheet

**CLASSIFICATION**

UNCLASSIFIED

**SYSTEM NUMBER**

127365



**TITLE**

DATA SELECTION FOR FAST PROJECTION TECHNIQUES: A COMPARATIVE STUDY OF  
DIRECTION FINDING PERFORMANCE

**System Number:**

**Patron Number:**

**Requester:**

**Notes:**

**DSIS Use only:**

**Deliver to:** HP



93-00117



National  
Defence

Défense  
nationale



UNLIMITED

**DATA SELECTION FOR FAST PROJECTION TECHNIQUES:  
A COMPARATIVE STUDY OF  
DIRECTION FINDING PERFORMANCE (U)**

by

**Mylène Toulgoat and Ross M. Turner**

**DEFENCE RESEARCH ESTABLISHMENT OTTAWA**  
REPORT NO. 1135

Canada

December 1992  
Ottawa





National    Défense  
Defence    nationale

**DATA SELECTION FOR FAST PROJECTION TECHNIQUES:  
A COMPARATIVE STUDY OF  
DIRECTION FINDING PERFORMANCE (U)**

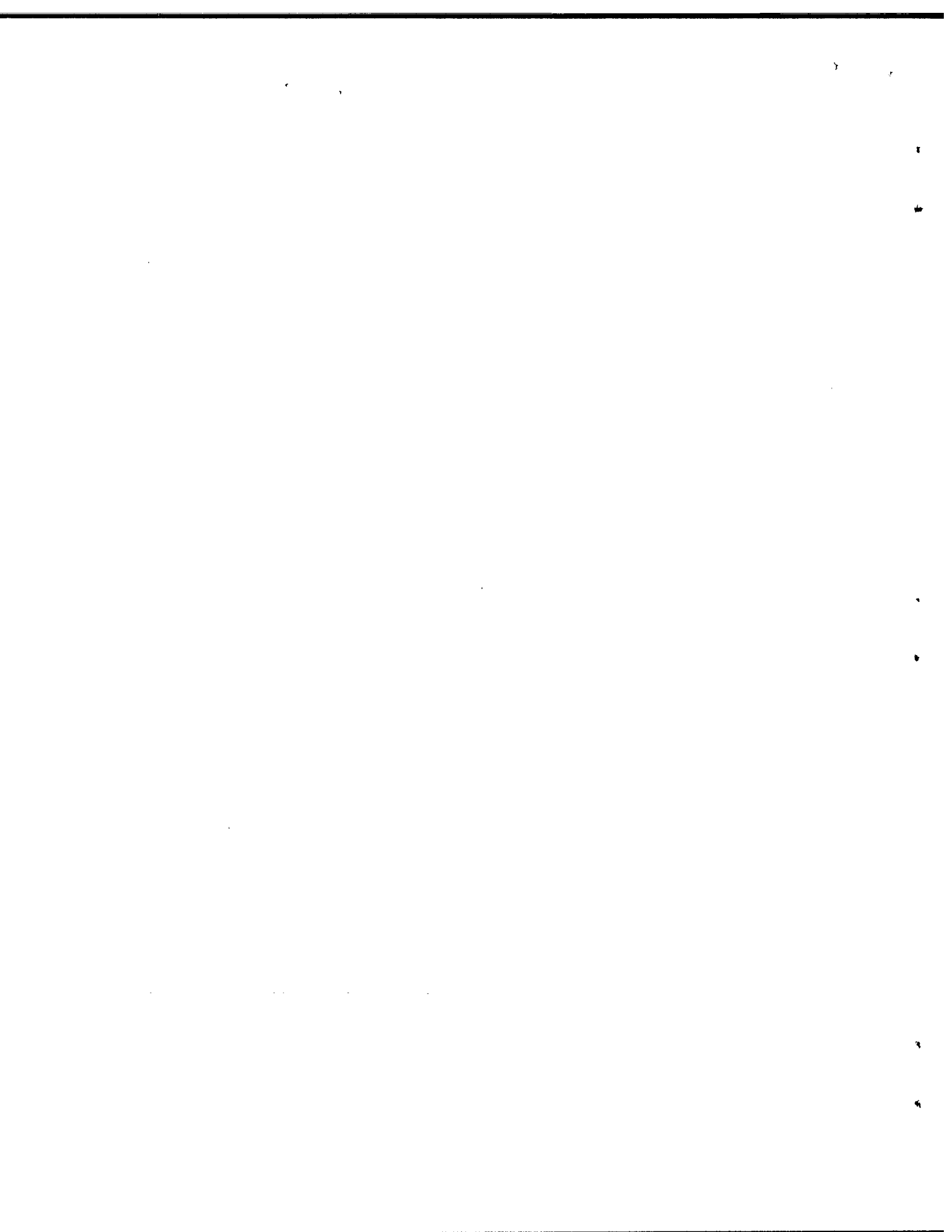
by

**Mylène Toulgoat and Ross M. Turner**  
*Surface Radar Section*  
*Radar Division*

**DEFENCE RESEARCH ESTABLISHMENT OTTAWA**  
REPORT NO. 1135

PCN  
041LC

December 1992  
Ottawa



# **DATA SELECTION FOR FAST PROJECTION TECHNIQUES: A COMPARATIVE STUDY OF DIRECTION FINDING PERFORMANCE**

by

**Mylène Toulgoat and Ross M. Turner**

## **ABSTRACT**

This report describes simulation studies of fast projection techniques for direction finding of jammer signals. These techniques are based on a data selection criterion applied directly to the data vectors obtained at the output of an antenna array. The selected data vectors are used in fast projection algorithms to estimate the jamming signal subspace and then to calculate the directional spectrum. Three such algorithms are described ranging from the fastest but least effective to the most computationally demanding but most effective. These algorithms provide a better trade-off of performance versus computational load than has heretofore been available. Relative performance is compared with that of the MUSIC technique for test cases which evaluate the minimum resolution threshold achievable and the effect of the jammer strength relative to the receiver noise.

## **RESUME**

Ce rapport est une étude, basée sur des simulations, de la performance relative des techniques de projection rapides pour trouver la direction de brouilleurs. Ces algorithmes utilisent un critère pour la sélection de bons vecteurs de données à la sortie d'une antenne réseau. Les vecteurs sélectionnés sont utilisés dans des algorithmes de projection rapides afin d'estimer le sous-espace des brouilleurs et ainsi calculer l'estimateur spectral. On décrit trois algorithmes le premier étant plus efficace du point de vue du nombre de calculs mais moins performant du point de vue du pouvoir de résolution, le dernier étant moins rapide mais plus performant. Ces algorithmes donnent un meilleur compromis entre le rendement et la charge de calculs que les algorithmes connus jusqu'à présent. On a comparé le rendement de ces trois techniques avec celui de la technique MUSIC pour deux scénarios différents qui évaluent le pouvoir de résolution et l'effet de la puissance des brouilleurs.





## EXECUTIVE SUMMARY

Accurate angular location and resolution of jamming sources is important for military sensor systems such as ESM and radar. This report describes three techniques for processing the outputs of antenna arrays to produce improved performance. Specifically, this report describes and evaluates computationally efficient algorithms for direction finding; these reduce the requirement for high speed computation and hence the cost of implementation.

The algorithms to be described and evaluated are based on projection techniques; the jamming signal subspace is estimated from the data vectors obtained from the antenna array elements. The jamming signal subspace is then used to calculate the directional spectrum, which basically consists of calculating the power of the projection of the search vector into the subspace orthogonal to the jamming signal subspace. As the search vector gets closer to the jammer direction, the power of the projected vector decreases. By taking the inverse of the projected power we obtain a directional spectrum with the peak positions reflecting the jammer directions.

Three algorithms, all based on data selection criteria followed by Gram-Schmidt orthogonalization, are described and evaluated. The algorithms are named as follows: (1) DVO for data vector orthogonalization, (2) DVSO for data vector selection and orthogonalization, (3) DVSO-COVAR for repeated applications of DVSO followed by a combining of the selected data vectors into a covariance matrix which in turn is followed by a final application of DVSO to the columns of the covariance matrix.

The above three algorithms are evaluated by means of simulations and compared with the standard MUSIC technique (MUSIC stands for Multiple Signal Classification). The latter is very computationally demanding. In terms of performance versus computational load, all three techniques compare favourably with the MUSIC technique. The three techniques trade off performance against computational load, DVO being the fastest in terms of computations but providing poorest resolution capability while DVSO-COVAR provides best resolution capability but at a cost of a considerable computational load.



## CONTENTS

1.0 INTRODUCTION .....	1
2.0 SIGNAL MODEL .....	2
3.0 PERFORMANCE EVALUATION .....	2
3.1 Monte-carlo simulations .....	2
3.2 Performance measures .....	3
3.2.1 Directional spectrum .....	3
3.2.2 Minimum resolution threshold .....	3
3.2.3 Error in the estimation of directions .....	4
3.3 Test cases .....	4
3.3.1 Test case $T_1$ .....	4
3.3.2 Test case $T_2$ .....	4
4.0 DATA VECTOR ORTHOGONALIZATION .....	5
4.1 Computational load .....	6
4.2 Computer simulations .....	6
5.0 DVSO TECHNIQUE .....	7
5.1 Computational count .....	8
5.2 Computer simulations .....	9
6.0 COMPARISON OF DVO AND DVSO .....	9
7.0 DVSO FOR ESTIMATING THE COVARIANCE MATRIX .....	12
7.1 Computer simulations .....	13
8.0 COMPARISON OF DVSO AND DVSO-COVAR .....	16
9.0 COMPARISON WITH MUSIC .....	18
9.1 Description of music technique .....	18
9.2 Computational load .....	19
9.3 Simulation results .....	20
10.0 CONCLUSIONS .....	22
11.0 REFERENCES .....	23



# DATA SELECTION FOR FAST PROJECTION TECHNIQUES: A COMPARATIVE STUDY OF DIRECTION FINDING PERFORMANCE

## 1.0 INTRODUCTION

Modern signal processing techniques provide the capability for very high-resolution determination of angles-of-arrival. While the performance of these techniques is very good, they have very high computational loads, precluding their use in many circumstances. Projection techniques based on eigenanalysis form the basis of the best performing and most popular high-resolution array signal-processing techniques. Such techniques have been used for angle-of-arrival estimation, for example the MUSIC technique of Schmidt [1] and the equivalent formulations of Bienvenu [2], as well as for adaptive antenna nulling of jammers [3,4]. Fast projection techniques, based on direct orthogonalization of the data vectors, avoid time consuming eigenanalysis but with some necessary loss of performance [5,6,7,8]. Toulgoat and Turner [9,10] have introduced aspects of data-vector selection to obtain a better trade-off between performance and speed for adaptive nulling of jamming signals.

This report is an evaluation of the fast projection methods of Toulgoat and Turner as applied to high-resolution direction finding similar to the evaluation carried out for adaptive nulling in [10]. As in [10], we consider a family of techniques starting with the fastest but poorest performing and progressing to the slowest but best performing. We consider three techniques: DVO for Data Vector Orthogonalization; DVSO for Data Vector Selection and Orthogonalization; and DVSO-COVAR, where DVSO is first used, the selected vectors are then formed into a covariance matrix, and DVSO is then applied to the columns of the covariance matrix. The data vectors selection technique used in DVSO-COVAR is similar to a technique of Reilly and Law [11]. However, [11] applies the selection process to the permutation and selection of columns of a covariance matrix. In contrast, we apply the data selection prior to the calculation of the covariance matrix in order to choose the data vectors used in the formation of the covariance matrix and then apply a procedure which is equivalent to that of [11] for selecting a subset of the columns vectors of the covariance matrix. The major contributions of this report are the new algorithms and the evaluation of their performance as a function of computational load for direction finding.

The basis of the evaluation is the resolution performance achieved versus the computational load as determined using Monte-Carlo simulations. In order to have a consistent measure of resolution performance, we define two signals as being resolved when the estimator has two peaks indicating the two signals near the true signal positions and where there is a dip of at least 3 dB between the peaks. The minimum resolution threshold is then the angular separation between the signals when this criterion is just satisfied. The evaluation is carried out for two test cases:  $T_1$  where the resolution threshold is determined for fixed and high signal-to-noise ratio; and  $T_2$  where the effect of different signal-to-noise ratios on the directional spectrum is examined. The three techniques are compared among themselves as to their performance versus computational loading. The final comparison is then made with the MUSIC algorithm.

## 2.0 SIGNAL MODEL

In this report, we consider only a uniform linear array with equally spaced elements. However, the techniques developed are also applicable to arbitrarily shaped arrays of non-uniformly spaced elements. The signals of interest comprise jamming interference received by the radar system. Such signal sources can be considered to be completely uncorrelated. The objective is to resolve these sources and to accurately determine their directions.

Radar systems are usually narrow band; this means that the received signal wave front has nearly perfect spatial correlation over the face of the array, provided that the time taken to cross the array is small compared with the reciprocal of the system bandwidth. The  $n^{\text{th}}$  data vector at time  $t_n$  is expressed as :

$$\mathbf{x}_n = \sum_{i=1}^L j_i(t_n) \mathbf{a}_i + \mathbf{n}_n$$

where  $L$  is the number of signals,  $\mathbf{n}_n$  is a receiver-noise vector with mutually independent components and power,  $E\{|\mathbf{n}_n|^2\} = K \sigma^2$ , with  $K$  the number of array elements. The quantity  $j_i(t_n)$  is a complex Gaussian random variable representing the  $i^{\text{th}}$  signal amplitude at time  $t_n$ , and  $\mathbf{a}_i$  is a deterministic vector representing the direction of arrival of the  $i^{\text{th}}$  signal defined as

$$\mathbf{a}_i = [1, \exp(j2\pi d \sin(\theta_i)/\lambda), \dots, \exp(j2\pi d(K-1) \sin\theta_i/\lambda)]^T$$

Here  $d$  is the inter-element spacing, and  $\theta_i$  is the direction of arrival of the  $i^{\text{th}}$  signal. The sample vectors or "snapshots" are taken at time intervals such that  $j_i(t_n)$  and  $j_i(t_{n-1})$  are completely independent.

## 3.0 PERFORMANCE EVALUATION

### 3.1 MONTE-CARLO SIMULATIONS

Monte-Carlo simulations are used to evaluate the performance of the various techniques. One hundred independent trials are carried out for each parameter setting under test with performance measures averaged over these trials. The jamming signals are generated as samples of a zero-mean complex Gaussian variate having perfect spatial correlation over the array and zero temporal correlation from one data vector to the next. This gives rise to a signal amplitude that is Rayleigh distributed. Receiver noise is also generated as samples of a zero-mean complex Gaussian variate but having zero spatial correlation over the array and zero temporal correlation from one data vector to the next. The receiver noise power at the element level is set at  $\sigma^2 = 10^{-4}$ .

The results are presented for ten-element and forty-element arrays of omnidirectional elements with an element spacing of one half wavelength.

## 3.2 PERFORMANCE MEASURES

### 3.2.1 DIRECTIONAL SPECTRUM

The directional spectrum  $F(\theta)$  used for angle-of-arrival estimation is given as

$$F(\theta) = \frac{1}{\mathbf{s}(\theta)^H \mathbf{P} \mathbf{s}(\theta)} \quad (1)$$

where  $\mathbf{P}$  is the projection matrix

$$\mathbf{P} = \mathbf{I} - \sum_{m=1}^M \mathbf{v}_m \mathbf{v}_m^H \quad (2)$$

$\mathbf{s}(\theta)$  is defined as

$$\mathbf{s}(\theta) = \frac{1}{\sqrt{K}} [1, \exp(j \frac{2\pi d}{\lambda} \sin\theta), \dots, \exp(j \frac{2\pi (K-1) d}{\lambda} \sin\theta)]^T$$

$d$  is the spacing between array elements,  $\lambda$  is the signal wavelength and  $\theta$  is the angle searched.

The entire space is searched, using low-resolution Fourier beamforming prior to the application of high-resolution spectral estimation to localize the regions of interest. This procedure is used to reduce the number of directions (denoted by  $n_d$ ) that are investigated. The present state of the art permits a resolution of about  $\frac{1}{4}$  of a beamwidth. The minimum number of directions to be searched is therefore  $n_d=4$  directions within a beamwidth. In practice however, the number may not be large enough to resolve the peak positions. In this report, we consider  $n_d=23$ . This value is larger than what might be needed in practice; however, such a large value of  $n_d$  suits our purpose: to show that the fast projection algorithms can be used for direction finding and to compare their resolution with that of the MUSIC method.

### 3.2.2 MINIMUM RESOLUTION THRESHOLD

The performance measure used is the minimum resolution threshold,  $\Delta\theta_{\min}$ , for two uncorrelated stochastic signals having the same Signal-to-Noise Ratio (SNR). Here the term SNR indicates the ratio of the power of the signal to the power of the receiver noise measured at the element receiver output. In each simulation trial, the two sources were considered resolved if they met the two following requirements:

- a) The spectral output of the algorithm under test had two peaks at or near the true source locations. An error of  $\pm(\theta_2-\theta_1)/10$  in location was allowed.
- b) The peaks at  $\theta_1$  and  $\theta_2$  were more than 3 dB above the value of  $F(\theta)$  at  $\theta=\theta_i \pm \Delta\theta/2$ , where  $i=1,2$  and  $\Delta\theta=\theta_2-\theta_1$ .

This measure of angular resolution is given in beamwidths (BW). One beamwidth is defined as  $\lambda/D$  where  $\lambda$  is the signal wavelength and  $D$  is the antenna aperture.

### 3.2.3 ERROR IN THE ESTIMATION OF DIRECTIONS

Since the data vectors contain receiver noise in addition to signals, the estimate of the signal subspace is not perfect. This causes error in the determination of signals directions. As seen in 3.2.2, an error of  $\pm\Delta\theta/10$  was allowed in the calculation of the minimum resolution threshold. To determine this error more precisely, we calculate the value of  $F(\theta)$  at intervals of  $\Delta\theta/100$  to obtain a precision of 1% of  $\Delta\theta$ . If, for example, we observe a peak at  $\theta_1 + 3\Delta\theta/100$ , we conclude that the position is off by 2.5 to 3.5% of the angle separation,  $\Delta\theta$ .

## 3.3 TEST CASES

We have specified two test cases,  $T_1$  and  $T_2$ , which are designed to determine the minimum threshold resolution,  $\Delta\theta_{\min}$ , achieved by the various techniques and to test the effect of the signal strength on the directional spectrum, respectively.

### 3.3.1 TEST CASE $T_1$

Here we have specified the Signal-to-Noise Ratio, SNR, at the receiving element output to be 40 dB. The number of signals is designated as  $L=2$ . The first signal is set at  $\theta_1=20^\circ$  while the second signal direction is at  $\theta_2=\theta_1+\Delta\theta$ . The separation  $\Delta\theta$  is then reduced until the threshold resolution,  $\Delta\theta_{\min}$ , is reached.

### 3.3.2 TEST CASE $T_2$

Here we have defined two equi-powered signals at  $\theta_1=20^\circ$  and  $\theta_2=30^\circ$ . We consider four values of SNR of 10, 20, 30 and 40 dB as measured at the element level. This test case is used to examine the performance of the various estimators as a function of SNR.



#### 4.0 DATA VECTOR ORTHOGONALIZATION

The Data Vector Orthogonalization (DVO) technique is an efficient method for constructing a basis for the (jamming) signal subspace and computing the corresponding directional spectrum  $F(\theta)$ . A set of  $M$  basis vectors,  $\{\mathbf{v}_m\}$ , is generated directly from a set of sample vectors,  $\{\mathbf{y}_m: m=1 \text{ to } M\}$ , selected from a larger group of  $N$  data vectors,  $\{\mathbf{x}_n: n=1 \text{ to } N\}$ , using the Gram-Schmidt (GS) orthonormalization method. Two thresholds are included in the procedure: an internal threshold  $\Delta$  that rejects data vectors which provide little additional information about the jamming signal subspace and an external threshold,  $\Delta_T$ , which forces the continued collection of data vectors and provides a termination criterion for the algorithm. The use of an external threshold in this manner was proposed by Nickel [7].

The  $m^{\text{th}}$  basis vector  $\mathbf{v}_m$  is generated from the  $n^{\text{th}}$  data vector  $\mathbf{x}_n$  using

$$\mathbf{u}_m = \mathbf{x}_n - \sum_{j=1}^{m-1} (\mathbf{v}_j^H \mathbf{x}_n) \mathbf{v}_j$$

We then compare the squared magnitude of  $\mathbf{u}_m$  to an internal threshold given by  $\Delta = 2K\sigma^2$ . The objective is to eliminate data vectors whose information content is too low. If  $|\mathbf{u}_m|^2 > \Delta$ , then  $\mathbf{u}_m$  is accepted and a new basis vector,  $\mathbf{v}_m$ , is generated as  $\mathbf{v}_m = \mathbf{u}_m / |\mathbf{u}_m|$ . If  $\mathbf{u}_m$  is not accepted, the procedure is started again with a new data vector  $\mathbf{x}_n$ .

Following the generation of  $\mathbf{v}_m$ , a statistic  $T$  is calculated as in [7]

$$T = \frac{\det(\mathbf{Y}^H \mathbf{Y})^{\frac{1}{2m}}}{\prod_{i=1}^k |\mathbf{y}_i|^2}$$

and tested against an external threshold,  $\Delta_T$ . Matrix  $\mathbf{Y}$  is constructed with the  $m$  data vectors selected from  $\{\mathbf{x}_n\}$ :

$$\mathbf{Y} = [\mathbf{y}_1, \mathbf{y}_2, \dots, \mathbf{y}_m]$$

When  $T < \Delta_T$ , the signal subspace has been sufficiently well estimated and the procedure is stopped. Otherwise, the procedure continues with a new data vector,  $\mathbf{x}_n$ . The accuracy of the estimation of the signal subspace depends on the choice of  $\Delta_T$ . Indeed, there is a trade-off between the accuracy of the estimate and the computational load depending on the choice of  $\Delta_T$ . The number of data vectors,  $N$ , that are examined and the number,  $M$ , selected are random variables for a given threshold value,  $\Delta_T$ . The dependence of the computational load on  $N$  and  $M$  will be evaluated by means of Monte-Carlo simulations.

## 4.1 COMPUTATIONAL LOAD

The computational count comprises two terms: the first term,  $C_b$ , is associated with the calculation of the basis vectors  $\{\mathbf{v}_m\}$ ; the second term,  $C_{sc}$ , represents the number of complex multiplications required for the calculation of the directional spectrum  $F(\theta)$ .

In the DVO technique, we assume that  $N$  data vectors are used to compute  $M$  orthonormal vectors spanning the signal subspace. An upper bound to the number of complex multiplications required is then

$$C_{DVO} = C_b + C_{sc}$$

where

$$C_b = KN^2 - 0.5KN + 0.5KM + \frac{(N-1)(K+1)}{2}$$

and

$$C_{sc} = n_d M(K+0.5) \quad (3)$$

where  $n_d$  is the number of angles searched i.e. the number of points at which the directional spectrum,  $F(\theta)$ , is evaluated.

## 4.2 COMPUTER SIMULATIONS

We first determine the minimum resolution threshold,  $\Delta\theta_{\min}$ , of the DVO algorithm for arrays of 10 and 40 elements using test case  $T_1$ . Figure 1 shows the resolution threshold,  $\Delta\theta_{\min}$ , versus the external threshold  $\Delta_T$ . As  $\Delta_T$  increases, the accuracy of the estimate of the signal subspace decreases and therefore  $\Delta\theta_{\min}$  increases. The errors in the estimation of the directions of the sources vary between 0% and 6.5% of  $\Delta\theta$  ( $\Delta\theta = \Delta\theta_{\min}$  in this case) for both sources and both arrays.

Next, we analyze the effect of the signal strength. Figure 2 shows the directional spectrum  $F(\theta)$  versus  $\theta$  for a threshold  $\Delta_T = 0.5$  using test case  $T_2$ . The peak heights are proportional to the relative SNR for each signal. The error in estimating the directions is less than 0.5% of  $\Delta\theta$  for SNR of 20, 30 and 40 dB and is less than 1.5% of  $\Delta\theta$  for SNR=10 dB. Further computer simulations showed that as the signal strength increases, the minimum resolution threshold,  $\Delta\theta_{\min}$ , achieved, becomes lower. As an example, two sources at  $\theta_1 = 20^\circ$  and  $\theta_2 = 25^\circ$  are resolved with a threshold  $\Delta_T=0.5$  for SNR=40 dB but cannot be resolved even with a threshold  $\Delta_T=1 \times 10^{-8}$  if SNR=10 dB. In the latter case, it was not possible to find an estimate of the signal subspace sufficiently accurate. As expected, the accuracy of the estimate of the signal directions increases with SNR.

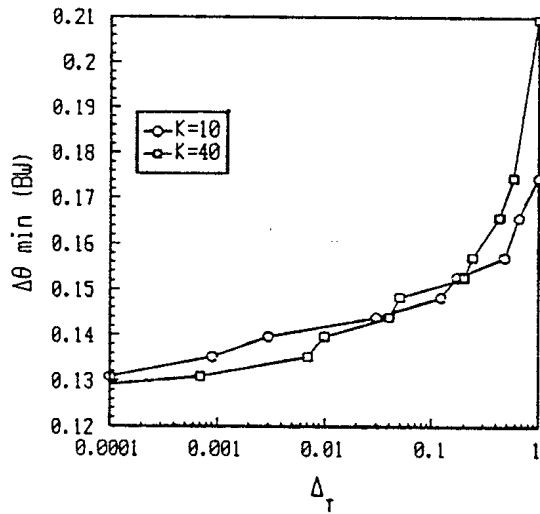


Fig. 1  $\Delta\theta_{\min}$  versus  $\Delta_T$  for DVO with  $L=2$  and  $\text{SNR}=40$  dB for arrays of 10 and 40 elements. Monte-Carlo simulations with 100 trials.

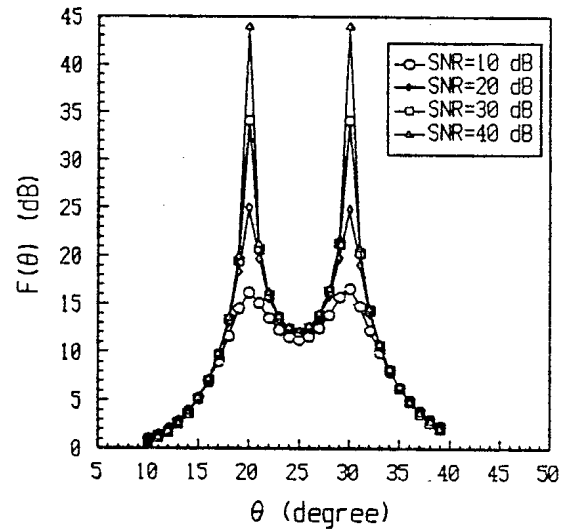


Fig. 2  $F(\theta)$  versus  $\theta$  for DVO with  $K=10$ ,  $L=2$ ,  $\Delta_T=0.5$ . Monte-Carlo simulations with 100 trials.

## 5.0 DVSO TECHNIQUE

The DVSO technique is based on a selection of the best  $M$  vectors from a larger group of  $N$  vectors which are sampled when only the jamming signals are present and stored before the process begins. The selected  $M$  vectors are best in the sense that they yield the most accurate estimate of the signal subspace as compared with any other set of  $M$  vectors selected from the larger set of  $N$ . In the algorithm for estimating the signal subspace, we use the following notation:  $\{\mathbf{x}_n\}$  comprises the set of  $N$  sample vectors,  $\{\mathbf{u}_m\}$  denotes the  $M$  best sample vectors chosen from the  $\{\mathbf{x}_n\}$ , and  $\{\mathbf{v}_m\}$  denotes the orthonormal basis formed from the  $\{\mathbf{u}_m\}$  by the GS method.

The data selection is integrated with the GS orthonormalization method. The data vector chosen has the largest projected amplitude in the subspace orthogonal to the previously selected  $(m-1)$  basis vectors  $\{\mathbf{v}_1, \dots, \mathbf{v}_m\}$ . The squared magnitude of this projection is

$$e_n^m = |\mathbf{P}_{m-1} \mathbf{x}_n|^2 \quad n=1, \dots, N$$

where  $\mathbf{P}_{m-1}$  is the projection matrix determined from the basis  $\{\mathbf{v}_1, \dots, \mathbf{v}_{m-1}\}$  as in equation (2). The iterations are initiated with  $\mathbf{P}_0 = \mathbf{I}$ , the identity matrix.

The  $m^{\text{th}}$  basis vector  $\mathbf{v}_m$  is generated from the  $n^{\text{th}}$  data vector  $\{\mathbf{x}_n\}$  using

$$\mathbf{u}_m = \mathbf{x}_n - \sum_{j=1}^{m-1} (\mathbf{v}_j^H \mathbf{x}_n) \mathbf{v}_j$$

We then compare the squared magnitude of  $\mathbf{u}_m$  to a threshold given by  $\Delta = 2K\sigma^2$ . If  $|\mathbf{u}_m|^2 > \Delta$  then  $\mathbf{v}_m = \mathbf{u}_m / |\mathbf{u}_m|$  and the process starts again with another data vector. Otherwise, the algorithm terminates with an estimate of the signal subspace given by  $\{\mathbf{v}_1, \dots, \mathbf{v}_M\}$  where  $M$  equals the final value of  $m$  in the iteration minus 1. The angle estimator is then obtained using equation (1).

## 5.1 COMPUTATIONAL COUNT

Although the concept of the projection matrix is central to the derivation of the technique, it is never explicitly calculated. It is computationally more efficient to work directly with the basis vectors. The projection matrix is only required in the selection of the data vector. We use the following properties of projection matrices to simplify the expression for  $\epsilon_n^m$ :

$$\mathbf{P}_{m-1}^H = \mathbf{P}_{m-1}$$

and

$$\mathbf{P}_{m-1} \mathbf{P}_{m-1} = \mathbf{P}_{m-1}$$

We can now write

$$\epsilon_n^m = \mathbf{x}_n^H \mathbf{P}_{m-1} \mathbf{x}_n = |\mathbf{x}_n|^2 - \sum_{k=1}^{m-1} |\mathbf{v}_k^H \mathbf{x}_n|^2$$

We obtain the iteration for  $\epsilon_n^m$  as

$$\epsilon_n^m = \epsilon_n^{m-1} - |\mathbf{v}_{m-1}^H \mathbf{x}_n|^2$$

With those simplifications, the computational load for the DVSO technique is given by:

$$C_{\text{DVSO}} = C_b + C_{\text{sc}}$$

where

$$C_b = K (0.5 + 0.5N + 2M + MN + M^2) + 0.5 MN$$

and  $C_{\text{sc}}$  is given by equation (3)

## 5.2 COMPUTER SIMULATIONS

We first determine the minimum resolution threshold,  $\Delta\theta_{\min}$ , for the DVSO technique using test case  $T_1$ . Figure 3 shows  $\Delta\theta_{\min}$  versus  $N$  for arrays of 10 and 40 elements. As  $N$  increases, the resolution threshold decreases down to a limit which is around 0.12 BW for  $K=10$  and 0.13 BW for  $K=40$ . Increasing  $N$  would slightly lower the minimum resolution threshold.  $N$  has been limited to 20 in the results presented here. It is observed that as  $K$  increases, the resolution in BW increases by a small amount. We then consider the error on the positions of the directions for the results of Figure 3. The error in estimating the source directions lies between 1.5% to 4.5% of  $\Delta\theta$  for  $\theta_1$  and 2.5% to 5.5% of  $\Delta\theta$  for  $\theta_2$  for both arrays, for  $\Delta\theta$  near the resolution limit,  $\Delta\theta_{\min}$ .

We next analyze the effect of signal strength on the directional spectrum. Figure 4 shows the directional spectrum  $F(\theta)$  versus  $\theta$  using test case  $T_2$  with  $N=5$  for SNR=10, 20, 30, 40 dB. The peaks of the function reflect the signal strength. Other computer simulations (results not given) showed that the height of the peaks is fairly insensitive to  $N$ , provided  $N$  is high enough to resolve the sources. It is also observed that the resolution threshold depends on the signal strength. As an example, for  $\theta_1=20^\circ$  and  $\theta_2=25^\circ$  we cannot find an  $N < 20$  for which the sources are resolved for SNR=10 dB but they are resolved with  $N=3$  for SNR=40 dB.

The error in estimating the signal directions has been determined for test case  $T_2$ . The results showed that the error is less than 1.5% of  $\Delta\theta$  for all SNR's. We observe from test cases  $T_1$  and  $T_2$  that, as the angle separation,  $\Delta\theta$ , increases, the error in the signal direction decreases.

## 6.0 COMPARISON OF DVO AND DVSO

Both the DVO and DVSO methods combine GS orthogonalization with a data selection process for the computation of the directional spectrum  $F(\theta)$ . In the DVO method, the data selection process consists of eliminating those data vectors which provide little additional information about the jamming signal subspace while continuing to take new sample vectors until a second external threshold criterion is satisfied. The data selection is carried out after the GS orthogonalization. In the DVSO technique, the data selection process consists of choosing the data vector which has the largest projected amplitude into the subspace orthogonal to the previously selected  $(m-1)$  basis vectors  $\{v_1, \dots, v_{m-1}\}$ . The data selection process of the DVO method is not as efficient as that of the DVSO method. In the DVO method, we eliminate data vectors that are not good enough while in DVSO we select the best data vectors. Therefore, the DVSO method gives a more accurate estimate of the signal subspace than does the DVO technique; the data selection criterion, however, requires more computations.

The curves of performance versus number of complex multiplications are obtained as follows: (1) for DVO we decrease the threshold,  $\Delta_T$ , which increases the number of calculations but gives better performance; (2) for DVSO we increase  $N$ , increasing the computational load and improving the resolution.

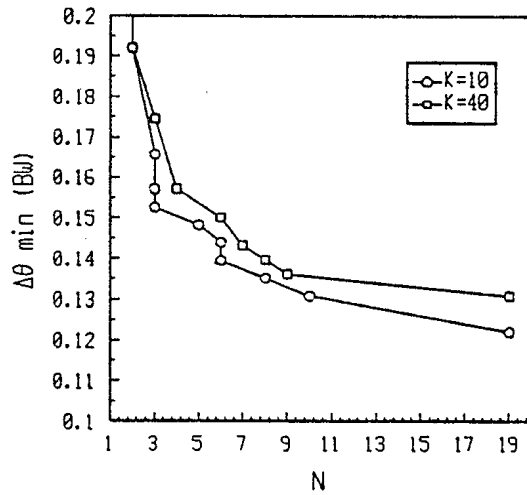


Fig. 3  $\Delta\theta_{\min}$  versus  $N$  for DVSO with  $L=2$ ,  $\text{SNR}=40$  dB. Monte-Carlo simulations with 100 trials.

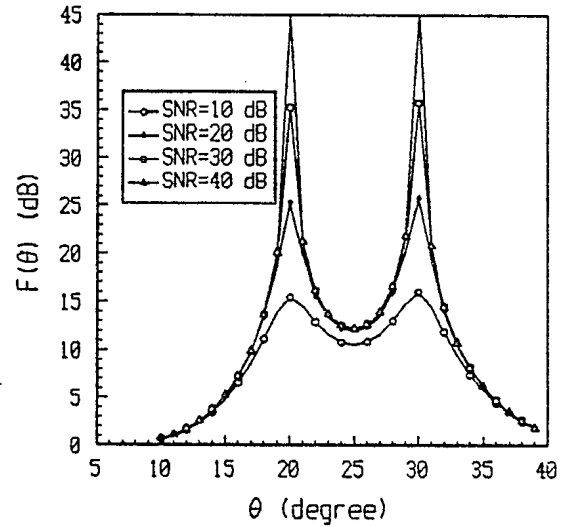


Fig. 4  $F(\theta)$  versus  $\theta$  for DVSO with  $K=10$ ,  $L=2$  and  $N=5$ . Monte-Carlo simulations with 100 trials.

Figure 5 shows the minimum resolution threshold,  $\Delta\theta_{\min}$ , versus complex multiplications for both DVO and DVSO techniques for an array of 10 elements. Two regions of operation are observed. Below  $\Delta\theta_{\min}=0.152$  BW, the DVSO method performs best in the sense that it requires less computations to provide a given  $\Delta\theta_{\min}$ . Above  $\Delta\theta_{\min}=0.152$  BW, the DVO method performs best. These results are obtained with  $n_d=23$  directions. Figure 6 gives the same performance for an array of 40 elements. We notice that there is no difference between DVO and DVSO for this array. Since the computational load is composed of two terms where only one term depends on the parameter  $n_d$ , it is interesting to plot  $\Delta\theta$  against the two terms separately. Figures 7 and 8 shows  $\Delta\theta_{\min}$  versus  $C_b$  and  $C_{sc}$ , respectively, for an array of 40 elements. From Figure 7, we see that the calculation of the basis by DVSO is more computationally intensive than that of the DVO method. Figure 8 shows that the search operation is less computationally intensive for DVSO when  $\Delta\theta_{\min}$  is less than 0.17 BW while requiring about the same number of computations as DVO for  $\Delta\theta_{\min}$  greater than 0.17 BW. Considering both terms of the computational load, the DVSO technique is advantageous for small values of  $\Delta\theta_{\min}$  and small arrays while both performs approximately the same as DVO for larger  $\Delta\theta$  and larger arrays.

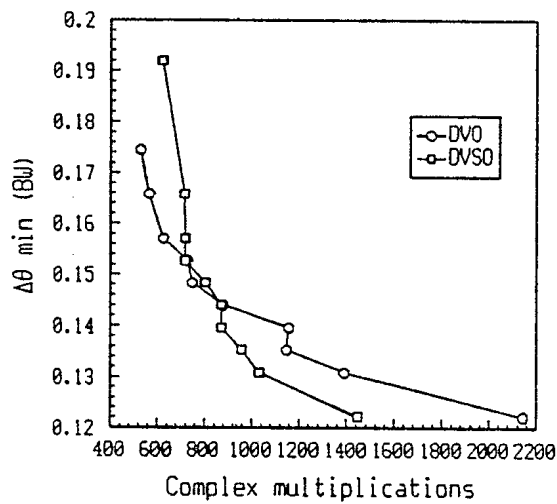


Fig. 5  $\Delta\theta_{\min}$  versus complex multiplications for DVO and DVSO with  $K=10$ ,  $L=2$  and  $SNR=40$  dB. Monte-Carlo simulations with 100 trials.

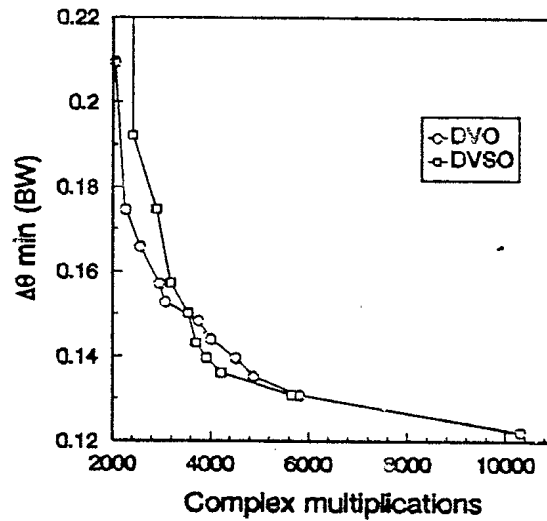


Fig. 6  $\Delta\theta_{\min}$  versus complex multiplications for DVO and DVSO with  $K=40$ ,  $L=2$  and  $SNR=40$  dB. Monte-Carlo simulations with 100 trials.

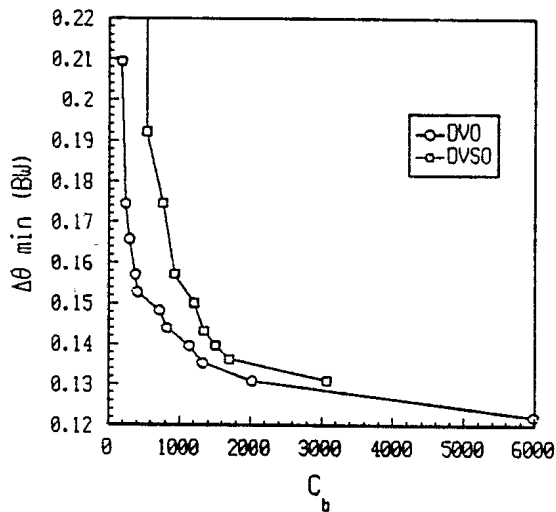


Fig. 7  $\Delta\theta_{\min}$  versus  $C_b$  for DVO and DVSO with  $K=40$ ,  $L=2$  and  $SNR=40$  dB. Monte-Carlo simulations with 100 trials.

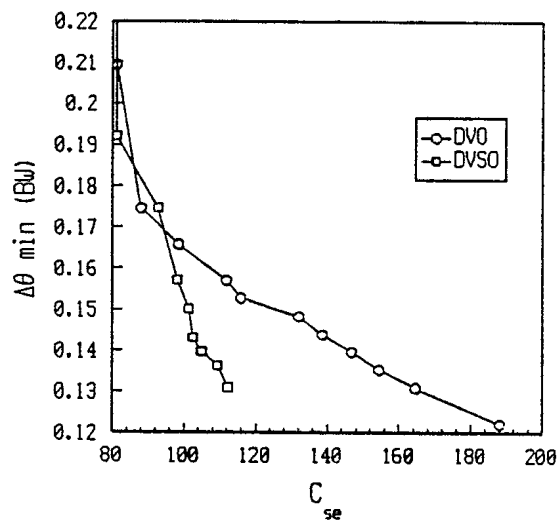


Fig. 8  $\Delta\theta_{\min}$  versus  $C_{se}$  for DVO and DVSO with  $K=40$ ,  $L=2$  and  $SNR=40$  dB. Monte-Carlo simulations with 100 trials.

## 7.0 DVSO FOR ESTIMATING THE COVARIANCE MATRIX

In this technique we employ the DVSO method twice. The first step is to subdivide a set of  $QN$  data vectors into  $Q$  groups of  $N$  vectors. DVSO is then applied to select the best  $M_i$  data vectors out of the  $i^{\text{th}}$  group,  $i=1$  to  $Q$ . This is repeated  $Q$  times to give

$$M_T = \sum_{i=1}^Q M_i$$

data vectors which are used to calculate the covariance matrix  $R$ :

$$R = \frac{1}{M_T} \sum_{i=1}^{M_T} \mathbf{x}_i \mathbf{x}_i^H$$

We are thus able to obtain an estimate of the covariance matrix using fewer but higher quality data vectors than in the conventional approach.

The final step applies the DVSO method to the columns of the covariance matrix to find an orthonormal basis and calculate a directional spectrum. This method is called DVSO-COVAR.

The data vector selection technique used is similar to a technique of Reilly and Law [11]. However, [11] applies the selection process to the permutation and selection of columns of a covariance matrix. In contrast we apply the criterion to the data vectors themselves thus reducing the number of data vectors used for computing the covariance matrix and therefore reducing the computational load. When we calculate the covariance matrix as in the DVSO-COVAR algorithm, the data vectors are subjected to the selection process before being combined in the covariance matrix. We then apply a procedure which is equivalent to that of [11] for selecting a subset of the columns vectors which are used to generate a basis for the signal space by means of the Gram-Schmidt process.

The number of computations required by the DVSO-COVAR technique is data-dependent; the mean number of calculations is estimated by Monte-Carlo simulations. For a single trial evaluation of the directional spectrum, the number of multiplications is

$$\sum_{i=1}^Q C_b(M_i, N, K) + \frac{M_T(K(K+1))}{2} + C_b(H, N, K) + C_{se}(H, K, n_d)$$

where  $C_b$  is the number of computations for the calculation of the basis by the DVSO technique and  $C_{se}$  is the number of computations for the evaluation of the directional spectrum;  $H$  is the number of basis vectors used to calculate the directional spectrum.



## 7.1 COMPUTER SIMULATIONS

We first analyze the effect of varying the parameters  $Q$  and  $N$  on the minimum resolution threshold  $\Delta\theta_{\min}$ . Figure 9 shows the minimum resolution threshold,  $\Delta\theta_{\min}$ , versus  $N$  for an array of 10 elements with  $Q=1,2,3$  and 4 using test case  $T_1$ . As for DVSO, increasing  $N$  lowers the minimum resolution threshold. This threshold is also lowered by increasing  $Q$ . For  $Q=1$ , the minimum resolution threshold is the same as that obtained for the DVSO technique while for  $Q=4$ ,  $\Delta\theta_{\min}$  can be as low as 0.09 BW. As in the DVSO technique,  $N$  is limited to 20. Figure 10 shows the minimum resolution threshold,  $\Delta\theta_{\min}$ , versus complex multiplications. We see that increasing  $Q$  decreases the minimum resolution threshold achieved but for a given  $\Delta\theta_{\min}$ , the computational load is about the same for the different values of  $Q$ . This can be explained by the fact that as  $Q$  increases, we need a lower  $N$  to achieve the same resolution. Therefore for small values of  $\Delta\theta_{\min}$ , there is no difference in the computational load. The error in estimating the directions of the sources for the results of Figure 10 (test case  $T_1$ ) lies between 0.5% to 6.5% of  $\Delta\theta$  for  $\theta_1$  and 1.5% to 5.5% of  $\Delta\theta$  for  $\theta_2$  (here  $\Delta\theta = \Delta\theta_{\min}$ ).

Figure 11 shows the minimum resolution threshold,  $\Delta\theta_{\min}$  versus  $Q$  for different values of  $N$  using test case  $T_1$  for an array of 10 elements. Increasing  $N$  for a given  $Q$  lowers the minimum resolution threshold. The decrease in  $\Delta\theta_{\min}$  obtained by increasing  $N$  is very small (less than 0.01 BW). Figure 12 shows  $\Delta\theta_{\min}$  versus complex multiplications for given values of  $N$  (the increase in the number of multiplications for a given  $N$  is due to the increase in the value of  $Q$ ). Up to a certain point, increasing  $N$  does not dramatically increase the computational load while permitting a better resolution. However, the curve of resolution versus calculation load quickly flattens out, so that a very high value of  $N$  does not provide a concomitant improvement in the resolution threshold. The bias of the estimates of signal directions varies from 1.5% to 6.5% of  $\Delta\theta$  for estimates of  $\Delta_1$  and from 2.5% to 6.5% of  $\Delta\theta$  for estimates of  $\theta_2$ .

We now compare the results obtained for  $K=10$  with those obtained for an array of 40 elements. Figure 13 shows  $\Delta\theta_{\min}$  in BW versus  $N$  for DVSO-COVAR,  $Q=4$  with  $K=10$  and  $K=40$  using test case  $T_1$ . The curves are quite similar even though the resolution in BW is slightly better for a smaller array.

Similarly, we plotted  $\Delta\theta_{\min}$  versus  $Q$  for DVSO-COVAR,  $N=5$  for arrays of 10 and 40 elements in Figure 14. The two curves lie on the top of each other.

We next analyze the effect of signal strength on the directional spectrum,  $F(\theta)$ , using test case  $T_2$ . Figure 15 shows  $F(\theta)$  versus  $\theta$  for  $Q=1$  and different values of SNR. The peaks reflect the signal strength with an offset of 5 dB. Figure 16 shows the directional spectrum  $F(\theta)$  versus  $\theta$  for SNR=40 dB and for different values of  $Q$ . As  $Q$  increases, the peaks become higher.

The position error is less than 0.5% of  $\Delta\theta$  for every value of SNR and  $Q$ . Moreover, the sharpness of the peaks increases with  $Q$  for a given SNR. Finally, the sharpness of the peaks increases with SNR for a given  $Q$ . As for DVSO, we conclude from test cases  $T_1$  and  $T_2$  that the error in the estimate of the signal directions decreases with increasing  $\Delta\theta$ .

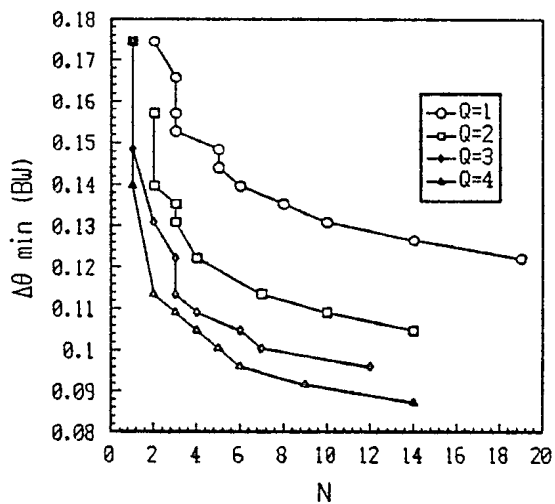


Fig. 9  $\Delta\theta_{\min}$  versus  $N$  for DVSO-COVAR with  $K=10$ ,  $L=2$  and  $\text{SNR}=40$  dB. Monte-Carlo simulations with 100 trials.

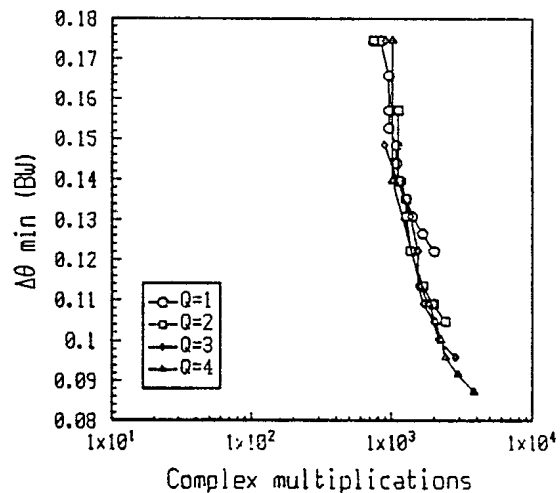


Fig. 10  $\Delta\theta_{\min}$  versus complex multiplications for DVSO-COVAR with  $K=10$ ,  $L=2$ ,  $n_d=23$  and  $\text{SNR}=40$  dB. Monte-Carlo simulations with 100 trials.

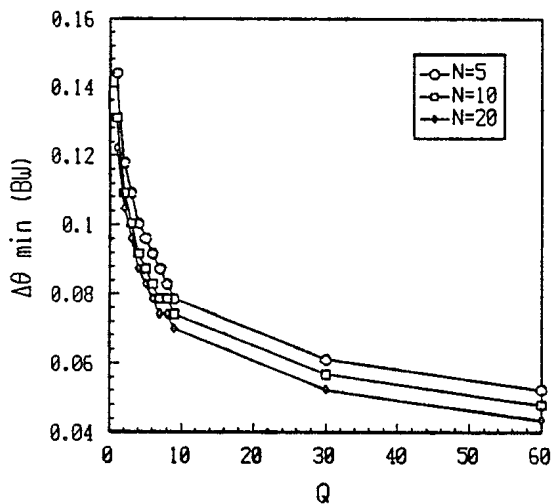


Fig. 11  $\Delta\theta_{\min}$  versus  $Q$  for DVSO-COVAR for  $N=5$ , 10 and 20 with  $K=10$ ,  $L=2$  and  $\text{SNR}=40$  dB. Monte-Carlo simulations with 100 trials.

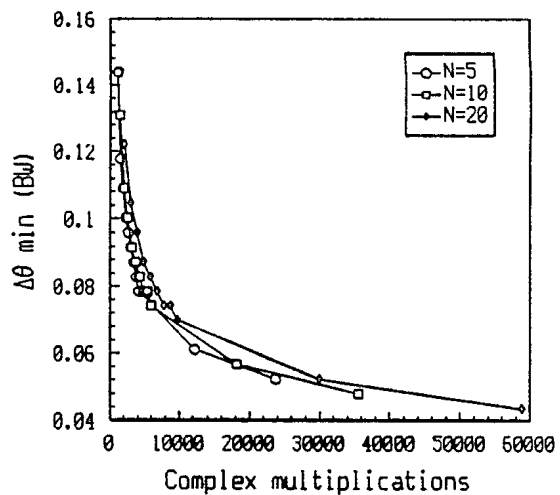


Fig. 12  $\Delta\theta_{\min}$  versus complex multiplications for DVSO-COVAR with  $K=10$ ,  $L=2$  and  $\text{SNR}=40$  dB. Monte-Carlo simulations with 100 trials.

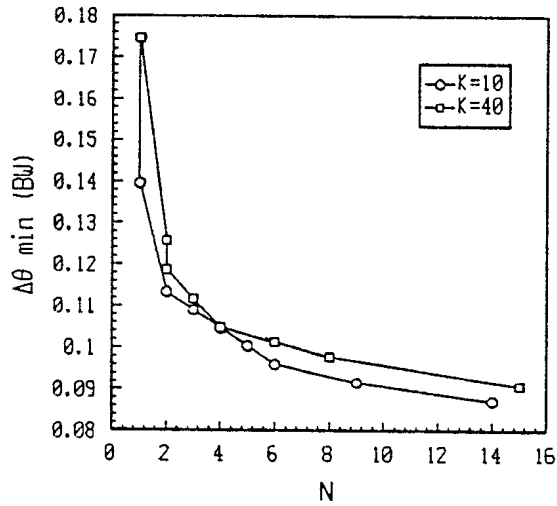


Fig. 13  $\Delta\theta_{\min}$  versus  $N$  for DVSO-COVAR with  $L=2$ ,  $Q=4$  and  $\text{SNR}=40$  dB. Monte-Carlo simulations with 100 trials.

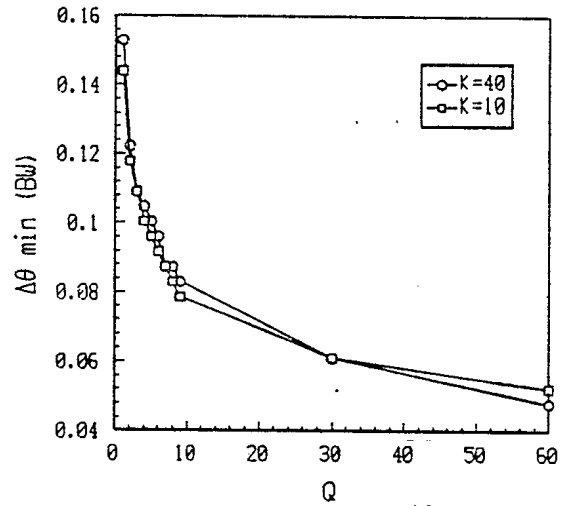


Fig. 14  $\Delta\theta_{\min}$  versus  $Q$  for DVSO-COVAR with  $L=2$ ,  $N=5$  and  $\text{SNR}=40$  dB. Monte-Carlo simulations with 100 trials.

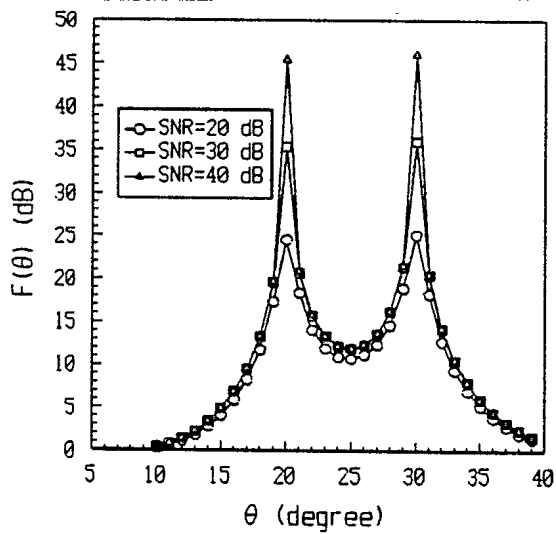


Fig. 15  $F(\theta)$  versus  $\theta$  for DVSO-COVAR with  $K=10$ ,  $L=2$ ,  $N=5$  and  $Q=1$ . Monte-Carlo simulations with 100 trials.

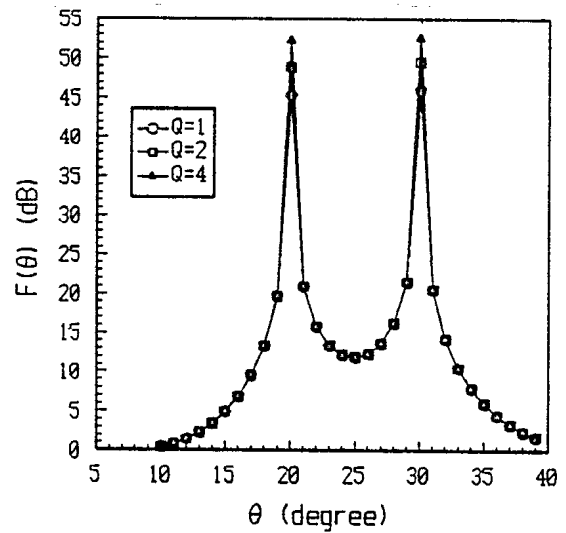


Fig. 16  $F(\theta)$  versus  $\theta$  for DVSO-COVAR with  $K=10$ ,  $L=2$ ,  $N=5$  and  $\text{SNR}=40$  dB. Monte-Carlo simulations with 100 trials.

## 8.0 COMPARISON OF DVSO AND DVSO-COVAR

We first compare the DVSO and DVSO-COVAR methods for test case  $T_1$  on the basis of their resolution versus computational load. Figure 17 shows  $\Delta\theta_{\min}$  versus complex multiplications for DVSO and DVSO-COVAR with  $n_d=23$  search directions for  $K=10$ . Two curves are shown for DVSO-COVAR: one for a fixed  $Q$  ( $Q=4$ ) with  $N$  varying, the other for fixed  $N$  ( $N=5$ ) with  $Q$  varying. There are two regions of operation: for  $\Delta\theta_{\min} > 0.124$  BW, DVSO performs best; for  $\Delta\theta_{\min} < 0.124$  BW, DVSO-COVAR performs best. From Figure 17 we see that DVSO-COVAR achieves a much lower resolution threshold by varying  $Q$  for a fixed  $N$  than by varying  $N$  for a fixed value of  $Q$ . Figure 18 shows  $\Delta\theta_{\min}$  versus the number of complex multiplications for both techniques with  $n_d=250$ . As  $n_d$  increases, DVSO-COVAR becomes slightly more efficient for low values of  $\Delta\theta_{\min}$ . For high values of  $\Delta\theta_{\min}$  where the value of  $N$  is at its smallest, the advantage of DVSO is evident. It should be noted however, that DVSO-COVAR can achieve a very high resolution - a resolution not achievable with DVSO - albeit at the cost of a considerable computational load. We next analyze the contribution of the terms  $C_b$  and  $C_{se}$  to the computational load. Figure 19 shows  $\Delta\theta_{\min}$  versus the number of complex multiplications required for the evaluation of the basis,  $C_b$ , for both techniques in the  $K=10$  case. As expected, the DVSO method is more computationally effective than DVSO-COVAR for the determination of the basis. Figure 20 shows  $\Delta\theta_{\min}$  versus the number of computations required for the evaluation of the directional spectrum,  $C_{se}$ , for the same techniques with  $n_d=23$ . Here we see that for low values of  $\Delta\theta_{\min}$ , DVSO-COVAR requires less computations than DVSO but for high values (above 0.2 BW) the number of computations required is the same.

Finally, Figure 21 shows the DVSO and DVSO-COVAR methods for  $K=40$  with  $n_d=23$  using test case  $T_1$ . For  $\Delta\theta_{\min}$  below 0.13 BW, DVSO-COVAR performs better while for  $\Delta\theta_{\min}$  above 0.13 BW the DVSO method performs better. We conclude that for direction finding, it is advantageous to use the DVSO method when only a moderate degree of superresolution is required. These conclusions are valid for a small number of signals such as  $L=2$ . It is likely that if the number of jammers,  $L$ , was increased in comparison to  $K$ , the DVSO-COVAR method would give better results.

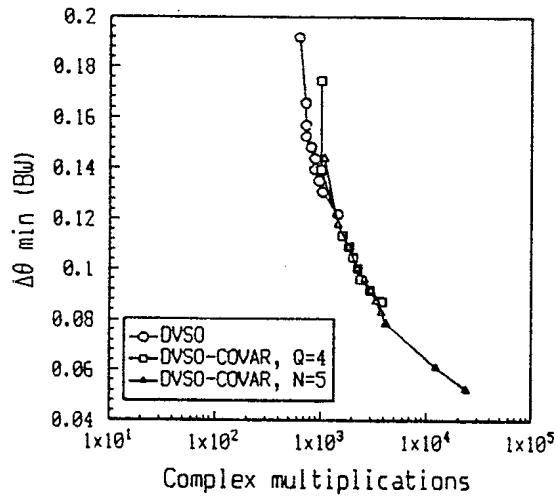


Fig. 17  $\Delta\theta_{\min}$  versus complex multiplications for DVSO and DVSO-COVAR with  $K=10$ ,  $L=2$ ,  $n_d=23$  and  $\text{SNR}=40$  dB. Monte-Carlo simulations with 100 trials.

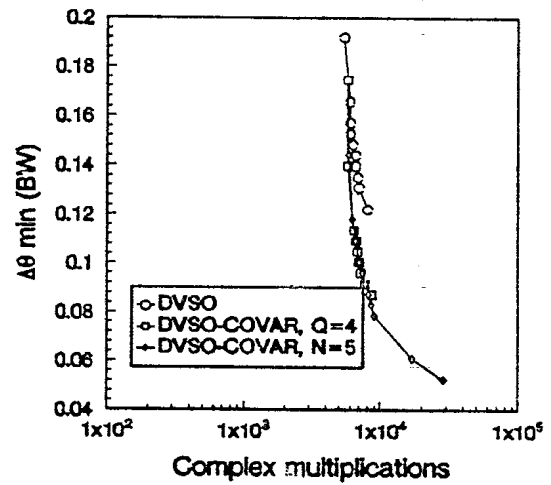


Fig. 18  $\Delta\theta_{\min}$  versus complex multiplications for DVSO and DVSO-COVAR with  $K=10$ ,  $L=2$ ,  $\text{SNR}=40$  dB and  $n_d=250$ . Monte-Carlo simulations with 100 trials.

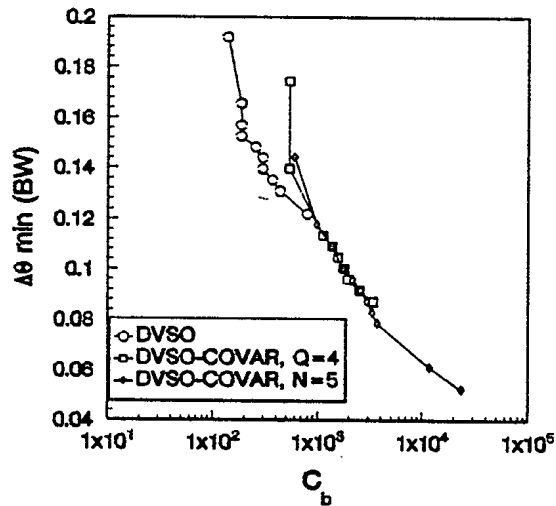


Fig. 19  $\Delta\theta_{\min}$  versus  $C_b$  for DVSO and DVSO-COVAR with  $K=10$ ,  $L=2$ ,  $\text{SNR}=40$  dB. Monte-Carlo simulations with 100 trials.

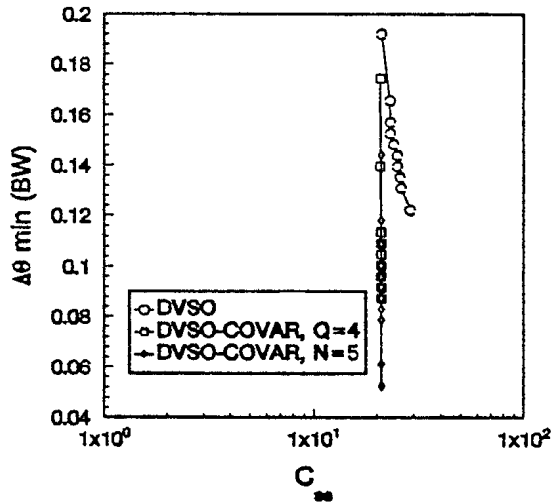


Fig. 20  $\Delta\theta_{\min}$  versus  $C_{sc}$  for DVSO and DVSO-COVAR with  $K=10$ ,  $L=2$ ,  $SNR=40$  dB. Monte-Carlo simulations with 100 trials.

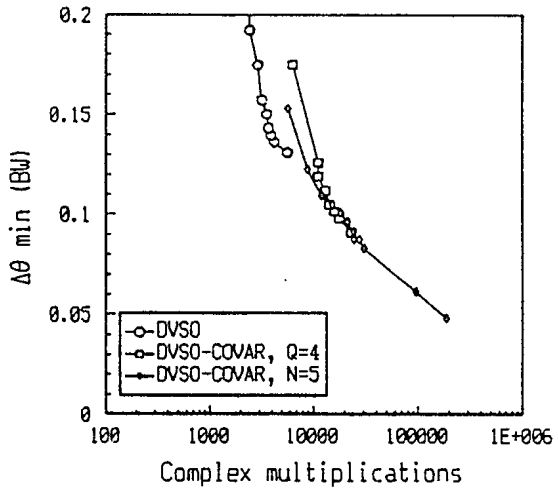


Fig. 21  $\Delta\theta_{\min}$  versus complex multiplications for DVSO and DVSO-COVAR  $Q=4$  with  $L=2$  and  $SNR=40$  dB. Monte-carlo simulations with 100 trials.

## 9.0 COMPARISON WITH MUSIC

Finally, we compare the fast projection techniques with the *MUSIC method*. Since we used a uniformly spaced linear array, the root-MUSIC technique [12] would have been a more appropriate choice but for the sake of generality we used the standard MUSIC technique because our techniques are also applicable to non-linear arrays.

### 9.1 DESCRIPTION OF MUSIC TECHNIQUE

In the MUSIC algorithm [1], the jamming signal subspace is constructed with the strongest eigenvectors of the covariance matrix. The covariance matrix is calculated from  $S$  data vectors as follows:

$$R = \frac{1}{S} \sum_{i=1}^S \mathbf{x}_i \mathbf{x}_i^H$$

where  $\mathbf{x}_i$  is the  $i^{\text{th}}$  data vector and  $S$  is the number of data vectors used in the calculation of the covariance matrix. This Hermitian matrix is decomposed in terms of its eigenvectors as

$$R = \sum_{i=1}^K \lambda_i \mathbf{v}_i \mathbf{v}_i^H$$

where  $\lambda_1 \geq \lambda_2 \geq \dots \geq \lambda_K$  is the set of ordered eigenvalues and  $\{\mathbf{v}_1, \dots, \mathbf{v}_K\}$  are the corresponding eigenvectors.

The Akaike Information Criterion (AIC) [13] is used to select the signal space eigenvectors. The number of these vectors is the  $p$  which minimizes the function:

$$AIC[p] = (K-p) \ln \frac{\frac{1}{K-p} \sum_{i=p+1}^K \lambda_i}{\prod_{i=p+1}^K \lambda_i^{\frac{1}{K-p}}} + p(2K-p)$$

## 9.2 COMPUTATIONAL LOAD

The expression for the computational load of the MUSIC technique comprises three terms. The first term,  $C_{cm}$ , is the number of computations required for the determination of the covariance matrix:

$$C_{cm} = \frac{S(K)(K+1)}{2}$$

where  $S$  is the number of data vectors used in the formation of the covariance matrix and  $K$  is the number of array elements. The second term,  $C_{ev}$ , is associated with the calculation of the eigenvalues and associated eigenvectors. A very efficient way to compute the eigenvalues of a complex Hermitian matrix (as the covariance matrix) employs Householder transformations to reduce the matrix to an equivalent symmetric tridiagonal matrix. The implicit QL algorithm [14] is then used to compute the eigenvalues of this tridiagonal matrix. The number of operations,  $C_{tr}$ , required for the tridiagonalization is given by

$$C_{tr} = \frac{2}{3}K^3 + \frac{3}{4}K^2 + \frac{25}{12}K - 7$$

Since the average number of iterations per eigenvalue is variable in the QL algorithm, we can only provide an approximate expression for the computations. The average number of iterations per eigenvalue is typically 1.3-1.6 [15]. We chose 1.3 for our calculation in order to obtain a lower bound on the computational load for MUSIC. Then the number of computations for the QL algorithm is

$$C_{QL} \approx 6K^2 - 3K$$

We then use the power method [15] to calculate the eigenvectors associated with the strongest eigenvalues. The number of operations required for the power method,  $C_{pow}$ , is

$$C_{pow} \approx 6K^2n_{ev} + 12Kn_{ev}^2 + 6f_s(n_{ev}^3) + 8n_{ev}^3$$

where  $n_{ev}$  is the number of eigenvectors to be calculated and  $f_s(n_{ev}^3)$  is the number of computations required for the full eigen solution of a  $n_{ev} \times n_{ev}$  matrix. We assumed that the eigenvectors are obtained after six iterations.

The total number of computations for the evaluation of the eigenvalues and eigenvectors is

$$C_{ev} = C_{tx} + C_{QL} + C_{pow}$$

The last term,  $C_{se}$ , is associated with the search of the peaks of the directional spectrum:

$$C_{se} = n_d p (K + 0.5)$$

The total computational load is then given by

$$C_{MUSIC} = C_{cm} + C_{ev} + C_{se}$$

In the next section we will show that the projection techniques compare favourably to the MUSIC technique.

### 9.3 SIMULATION RESULTS

We compared the DVSO, DVSO-COVAR and MUSIC techniques on the basis of test case T<sub>1</sub>. The performance of the MUSIC technique is shown in Figure 22;  $\Delta\theta_{min}$  is plotted versus  $S$  for arrays of 10 and 40 elements. As expected, the resolution threshold decreases as the number of data snapshots increases. The resolution performance of MUSIC as a function of computational load is compared with that of the fast projection techniques, DVSO and DVSO-COVAR, in Figure 23 and 26. Figure 23 shows  $\Delta\theta_{min}$  versus complex multiplications for both MUSIC and DVSO-COVAR techniques for an array of 10 elements. The DVSO method performs best for  $\Delta\theta_{min} > 0.12$  BW. The DVSO-COVAR technique performs best for  $0.09$  BW  $< \Delta\theta_{min} < 0.12$  BW. Below  $0.09$  BW the MUSIC technique performs best. Figure 24 shows  $\Delta\theta_{min}$  versus complex multiplications for an array of 40 elements. For  $\Delta\theta_{min} > 0.13$  BW, the DVSO technique performs best while for  $\Delta\theta_{min} < 0.13$  BW, the DVSO-COVAR perform best. As  $K$  increases, the region in which DVSO-COVAR performs better than MUSIC extends to much higher resolution, down to about  $0.04$  BW for a 40-element array; the performance advantage of DVSO over MUSIC in the intermediate resolution region also becomes more pronounced. It should be noted that very high resolutions (e.g.  $0.04$  BW) are usually considered



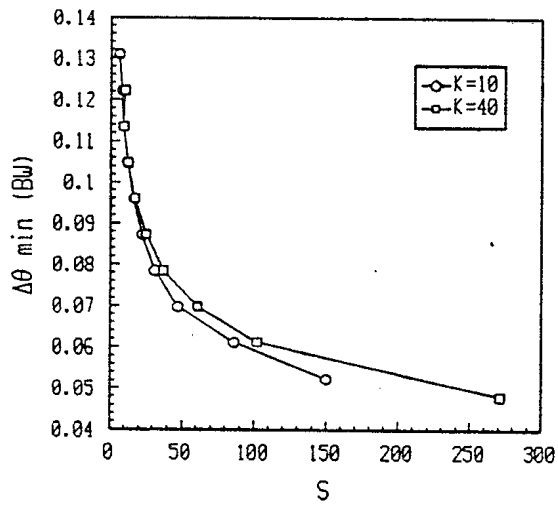


Fig. 22  $\Delta\theta_{\min}$  versus S for MUSIC with SNR=40 dB. Monte-Carlo simulations with 100 trials.

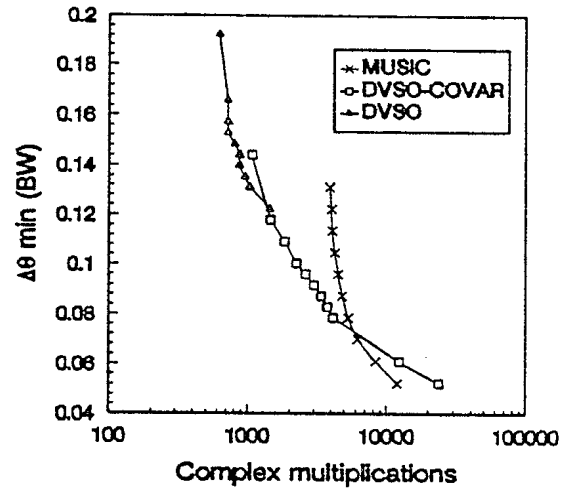


Fig. 23  $\Delta\theta_{\min}$  versus complex multiplications for MUSIC and DVSO-COVAR with K=10 and SNR=40 dB. Monte-Carlo simulations with 100 trials.

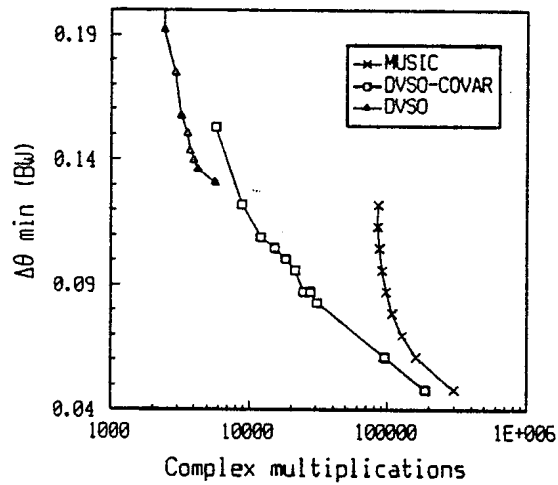


Fig. 24  $\Delta\theta_{\min}$  versus complex multiplications for MUSIC and DVSO-COVAR with K=40 and SNR=40 dB. Monte-Carlo simulations with 100 trials.

to be not practiced for MUSIC because of sensitivity to calibration errors in real antenna systems. The sensitivity of DVSO and DVSO-COVAR to calibration errors has not been evaluated and is beyond the scope of this study.

## 10.0 CONCLUSIONS

We have compared the performance of three projection methods, DVO, DVSO and DVSO-COVAR with the performance of MUSIC technique.

The selection of the best technique for a particular application is a function of the computational capability available and the degree of high resolution sought. The performance curves presented in this report allow a more nearly optimum trade-off between performance and computational load than has heretofore been available. Specifically, if a moderate degree of super-resolution is required, DVO provides the best combination of speed versus performance; a somewhat high degree of resolution leads to selection of DVSO; still higher resolution requires DVSO-COVAR with its high computational load. The above-mentioned fast projection techniques provide performance superior to that achievable with MUSIC in terms of resolution versus computational load - as long as the number of array elements,  $K$ , is high compared to the number of jammers  $L$ .

## 11.0 REFERENCES

1. Schmidt, R.O. "Multiple Emitter Location and Signal Parameter Estimation", IEEE Trans., Vol. AP-24, 1986, pp.276-280.
2. Bienvenu, G., Kopp, L., "Optimality of High Resolution Array Processing using the Eigensystem Approach", IEEE trans., vol. ASSP-31, No.5, october 1983, pp.1235-1247.
3. Bühring, W., "Adaptive Orthogonal Projection for Rapid Converging Interference Suppression", Electron. Lett., 1978, 14, pp. 515-516.
4. Bühring, W., "Adaptive Antenna with Rapid Convergence", IEE Conf. on Antennas and Prop., IEE Conf. Publ. 169, 1978, pp.51-54.
5. Hung, E.K.L., Turner, R.M., "A Fast Beamforming Algorithm for Large Arrays", IEEE Trans. Vol. AES-19, No-4, July 1983, pp.598-607.
6. Hung, E.K.L., Turner, R.M., Herring, R.W., "Fast and Effective Adaptive Beamforming and Spectral line Estimation by Direct Orthogonalization of the Data Vectors", IEEE Asilomar Conference on Circuits, Systems and Computers, Oct. 31 - Nov.2, 1983, pp.276-281.
7. Nickel, U., "Some Properties of Fast Projection Methods of the Hung-Turner Type", Signal Processing III: Theories and Applications, I.T. Young et al (eds.), North Holland, 1986, pp.1165-1168.
8. Nickel, U., "Angular superresolution by antenna array processing", International conf. on radar, Paris, April 24-28, 1989, pp. 48-58.
9. Toulgoat, M., Turner, R.M., "The Application of Sample Vector selection to Adaptive Nulling: Performance Comparison for Techniques Combining Gram-Schmidt Orthogonalization with Averaging", Canadian Conference on Electrical and Computer Engineering, Quebec, Sep. 25-27, 1991.
10. Toulgoat, M. and Turner, R.M., "Data Selection for Fast Projection Techniques Applied to Adaptive Nulling: A Comparative Study of Performance (U)", DREO Technical Report # 1100, Dec.1991.
11. Reilly, J.P. and Law, M.K., "A Fast High Performance Array Processing Technique for Angle-of-Arrival Estimation and Detection of the Number of Incident Signals", Canadian J. Elect. & Comp. Eng., Vol. 14, pp.38-45, 1989.

12. Barabell, A. J., "Improving the Resolution Performance of Eigenstructure Based Direction Finding Algorithms", ICASSP, Boston, MA, pp.336-339, 1983.
13. Wax, M. and T. Kailath, "Detection of Signals by Information Theoretic Criteria, IEEE Trans. Acoust. Speech Signal Process., vol. ASSP-33, pp. 387-392, April 1985.
14. Jennings, Alan, "Matrix Computation for Engineers and Scientists - Chap.10 ", John Wiley & Sons, Chichester, 1977, 330 p.
15. Press, W.H. et al., "Numerical Recipes in C", Cambridge University Press, Cambridge, 1988, pp.353-397.

**DOCUMENT CONTROL DATA**

(Security classification of title, body of abstract and indexing annotation must be entered when the overall document is classified)

1. ORIGINATOR (the name and address of the organization preparing the document. Organizations for whom the document was prepared, e.g. Establishment sponsoring a contractor's report, or tasking agency, are entered in section 8.)		2. SECURITY CLASSIFICATION (overall security classification of the document, including special warning terms if applicable)	
DEFENSE RESEARCH ESTABLISHMENT OTTAWA 3701 Carling ave, Ottawa, Ontario, K1A 0Z4		UNCLASSIFIED	
3. TITLE (the complete document title as indicated on the title page. Its classification should be indicated by the appropriate abbreviation (S,C or U) in parentheses after the title.)			
Data Selection for Fast Projection Techniques: a Comparative Study of Direction Finding Performance (U)			
4. AUTHORS (Last name, first name, middle initial)			
Toulgoat, Mylène and Turner, Ross M.			
5. DATE OF PUBLICATION (month and year of publication of document)		6a. NO. OF PAGES (total containing information. Include Annexes, Appendices, etc.)	6b. NO. OF REFS (total cited in document)
		28	15
7. DESCRIPTIVE NOTES (the category of the document, e.g. technical report, technical note or memorandum. If appropriate, enter the type of report, e.g. interim, progress, summary, annual or final. Give the inclusive dates when a specific reporting period is covered.)			
DREO Technical Report			
8. SPONSORING ACTIVITY (the name of the department project office or laboratory sponsoring the research and development. Include the address.)			
Defense Research Establishment Ottawa / Radar Division Ottawa, Ontario, Canada, K1A 0K2.			
9a. PROJECT OR GRANT NO. (if appropriate, the applicable research and development project or grant number under which the document was written. Please specify whether project or grant)		9b. CONTRACT NO. (if appropriate, the applicable number under which the document was written)	
041LC			
10a. ORIGINATOR'S DOCUMENT NUMBER (the official document number by which the document is identified by the originating activity. This number must be unique to this document)		10b. OTHER DOCUMENT NOS. (Any other numbers which may be assigned this document either by the originator or by the sponsor)	
DREO REPORT 1135			
11. DOCUMENT AVAILABILITY (any limitations on further dissemination of the document, other than those imposed by security classification)			
<input checked="" type="checkbox"/> Unlimited distribution <input type="checkbox"/> Distribution limited to defence departments and defence contractors; further distribution only as approved <input type="checkbox"/> Distribution limited to defence departments and Canadian defence contractors; further distribution only as approved <input type="checkbox"/> Distribution limited to government departments and agencies; further distribution only as approved <input type="checkbox"/> Distribution limited to defence departments; further distribution only as approved <input type="checkbox"/> Other (please specify):			
12. DOCUMENT ANNOUNCEMENT (any limitation to the bibliographic announcement of this document. This will normally correspond to the Document Availability (11). However, where further distribution (beyond the audience specified in 11) is possible, a wider announcement audience may be selected.)			

13. ABSTRACT (a brief and factual summary of the document. It may also appear elsewhere in the body of the document itself. It is highly desirable that the abstract of classified documents be unclassified. Each paragraph of the abstract shall begin with an indication of the security classification of the information in the paragraph (unless the document itself is unclassified) represented as (S), (C), or (U). It is not necessary to include here abstracts in both official languages unless the text is bilingual).

07011 This report describes simulation studies of fast projection techniques for direction finding of jammer signals. These techniques are based on a data selection criterion applied directly to the data vectors obtained at the output of an antenna array. The selected data vectors are used in fast projection algorithms to estimate the jammer subspace and then calculate the directional spectrum. Three such algorithms are described ranging from the fastest but least effective to the most computationally demanding but most effective. These algorithms provide a better trade-off of performance versus computational load than has heretofore been available. Relative performance is compared with that of the MUSIC technique for test cases which evaluate the minimum resolution threshold achievable and the effect of the jammer strength relative to the receiver noise. U

14. KEYWORDS, DESCRIPTORS or IDENTIFIERS (technically meaningful terms or short phrases that characterize a document and could be helpful in cataloguing the document. They should be selected so that no security classification is required. Identifiers, such as equipment model designation, trade name, military project code name, geographic location may also be included. If possible keywords should be selected from a published thesaurus. e.g. Thesaurus of Engineering and Scientific Terms (TEST) and that thesaurus-identified. If it is not possible to select indexing terms which are Unclassified, the classification of each should be indicated as with the title.)

DIRECTION FINDING  
FAST PROJECTION TECHNIQUES  
RADAR  
PHASED ARRAY

93-00117

JAN 22 1993

NO. OF COPIES NOMBRE DE COPIES	COPY NO. COPIE N°	INFORMATION SCIENTIST'S INITIALS INITIALES DE L'AGENT D'INFORMATION SCIENTIFIQUE
1	1	DAG
AQUISITION ROUTE FOURNI PAR	DREO	
DATE	21 JANUARY 1993	
DSIS ACCESSION NO. NUMÉRO DSIS	93-00117	

DND 1158 (6-87)

 National  
Defence

Défense  
nationale

# ~~124252~~  
127365